IMPROVED MICROCALCIFICATION DETECTION UTILIZING ENHANCEMENT TECHNIQUES

A.N. Papadopoulos*,** and D.I. Fotiadis**

* Dept. of Medical Physics, Medical School, University of Ioannina, GR 45110 Ioannina, Greece
** Dept. of Computer Science, Unit of Medical Technology and Intelligent Information Systems, University of Ioannina, GR 45110 Ioannina, Greece

me00236@cc.uoi.gr, fotiadis@cs.uoi.gr

Abstract: The aim of this study is to evaluate the influence of image enhancement techniques on a computer-aided detection system (CAD) used for the microcalcification detection in mammograms. The enhancement techniques which are utilized based on conventional and more sophisticated image analysis techniques. The contrast limited adaptive histogram equalization (CLAHE) and the local range modification (LRM) algorithms belong to the first category. In addition, techniques based on the 2-D redundant dyadic wavelet transformation (RDWT) are studied. Two mammographic datasets, the Mammographic Image Analysis Society (MIAS) and the Nijmegen databases are used for the evaluation of the CAD system performance. The highest detection performance is achieved by the enhancement algorithm LRM.
Keywords: **Mammography image enhancement, microcalcification detection, CAD**

Introduction

Mammography is a well-established method for the detection of breast cancer in its early stages. Microcalcification clusters are considered as a significant early sign of breast cancer. However, the complexity of the mammographic images due to the presence of multiple background and overlapping structures, makes its interpretation difficult. Although recent computer aided detection (CAD) schemes achieve high sensitivity levels, their performance could be further improved by utilizing preprocessing techniques.

Several mammogram preprocessing algorithms have been utilized in CAD systems. A methodology proposed by Pizer et. al. [1] is based on histogram equalization, which by the description of image contrast thresholds defines the contrast-limited adaptive histogram equalization (CLAHE) technique. Lure et. al. [2] employ an unsharp masking algorithm while Morrow et. al. [3] suggested a region-based approach named adaptive-neighborhood contrast enhancement which is based on the differentiation of foreground and background areas of the examined structure. Strickland et. al. [4] and Laine et. al. [5] have used discrete wavelet transforms (DWT) with biorthogonal spline filters. The selection of distinct decomposition levels produces enhanced mammographic versions. Fractal [6] and fuzzy logic [7] methodologies are also approaches resulting in sophisticated enhancement of breast images. However, mammogram enhancement techniques support not only CAD systems but they also result in improved quality images which can be viewed by the doctors. Such use of mammographic images is reported by Sivaramakrishna et. al. [8] in which a significant improvement in radiologist's detection score has been achieved with the utilization of several enhancement algorithms.

In this study, microcalcification enhancement schemes have been employed in the preprocessing stage of a CAD system [9]. The CLAHE technique and the local range modification (LRM) algorithm are two approaches based on spatial analysis and histogram equalization techniques. A 2-D redundant dyadic wavelet transform (RDWT) is utilized modifying the fraction of the coarseness and the detailed portion of the mammogram. By the selection of different image decomposition levels, the contrast of the initial mammogram is improved. In addition, wavelet coefficients are appropriately adjusted using linear stretching and wavelet shrinkage techniques. The performance of the CAD system is evaluated for the variant image enhancement techniques by the utilization of a receiver operating characteristic (ROC) analysis using two mammographic databases, the Mammographic Image Analysis Society (MIAS) and the Nijmegen database.

Materials and Methods

The adaptive histogram equalization algorithm is a well established contrast enhancement technique which has been utilized in several medical image applications [1]. It is based on the histogram equalization technique which applies in regions (blocks) of the original mammogram. However, due to specific weaknesses such as the intensity discontinuities at the block borders, it is replaced in most cases by the CLAHE methodology. CLAHE subdivides the image into $n \times m$ blocks, calculating the histogram of each such block. Every region is then equalized by choosing a monotonically nondecreasing gray level transformation, mapping the histogram of a desired distribution. However, the enhancement of a block is limited by the

ISSN: 1727-1983

selection of a clipping level, defined as a multiple of the histogram average. Those pixels exceeding the clip limit are equally redistributed across the histogram, their value being finally adjusted according to interpolation between the histograms of neighboring regions. The clipping factor can help, if properly adjusted, to reduce noise amplification in poorly contrasted areas.

The mapping function at each pixel is proportional to the local cumulative histogram. Contrast enhancement is proportional to the slope of the mapping function. For slope equal to one, no enhancement is achieved, while higher values of the slope result in image enhancement. In homogenous areas, the histogram exhibits high peaks and thus a narrow range of input grayscale values is mapped to a wider range of output grayscale values. In such a case, the noise in homogenous regions is over-enhanced. The limiting slope of the mapping function is determined by the user. The clipping limit C is S times the average histogram value, since a mapping function with a constant slope of one corresponds to all histogram values equal to the same average number of pixels. Thus, the critical parameter in the application of CLAHE algorithm is the definition of a clip limit which in our case is set equal to 0.5. After its selection, each histogram is redistributed so that its height does not exceed the clip limit.

Local range modification (LRM) [3] also utilized. In this method the output intensity of each pixel, z, is related with the input intensity of the pixel with the following relation:

$$z = aw + b, \tag{1}$$

where a and b are parameters which depend on local contrast.

Those parameters are calculated for overlapping blocks of the image and are then estimated by using interpolation for each pixel position. The spatially-dependent parameters of the image are first computed and afterwards these parameters are applied to the original mammogram. Thus, the original image is divided to non-overlapping blocks. The size of the block (s) is a parameter that depends on the resolution and structure of the image. The maximum and minimum grayscale values H_i and L_i are computed for each block. For the half-overlapping blocks having block size 2s the maximum and minimum grayscale values M_i and N_i are calculated. These values are the largest H_i and smallest L_i values, respectively, for the four s-sized blocks contained within each 2s-sized block.

The estimated local maximum and local minimum values for each pixel are calculated by interpolating the M_i and N_i values at the four surrounding grid points:

$$\begin{aligned}\max \;=\; & \left[\frac{s_y}{s}M_4 + \left(\frac{s-s_y}{s}\right)M_1\right]\left(\frac{s-s_x}{s}\right) + \\ & \left[\frac{s_y}{s}M_5 + \left(\frac{s-s_y}{s}\right)M_2\right]\frac{s_x}{s},\end{aligned} \tag{2}$$

$$\begin{aligned}\min \;=\; & \left[\frac{s_y}{s}N_4 + \left(\frac{s-s_y}{s}\right)N_1\right]\left(\frac{s-s_x}{s}\right) + \\ & \left[\frac{s_y}{s}N_5 + \left(\frac{s-s_y}{s}\right)N_2\right]\frac{s_x}{s},\end{aligned} \tag{3}$$

where s_x ,and s_y are the horizontal and vertical distances of the sample point, respectively from the (M_1,N_1) grid point, M_1, M_2, M_4, M_5 and N_1, N_2, N_4, N_5 are the maximum and minimum intensity values of the four surrounding grid points. The output value for each pixel is then calculated by linear stretching, using the local maximum and local minimum values:

$$y[m,n] = \frac{L-1}{(\max - \min)}(x[m,n] - \min), \tag{4}$$

Linear stretching rescale the local input grayscale range (min,max) to the full available $(0,L-1)$ grayscale range where L is the number of available output grayscale levels. The critical parameter in LRM is the local neighborhood length which corresponds to the block size. We selected the 51×51 pixels block size which provided the highest sensitivity to the detection of microcalcification.

The wavelet transform which is employed is a 2-D redundant - overcomplete dyadic wavelet transform [5]. This transformation is actually a uniform sampling of a corresponding 2-D Continuous Wavelet Transform which uses two oriented prototype wavelet functions $\psi^1(x,y)$,$\psi^2(x,y)$ given by:

$$\psi^1(x,y) = \frac{\partial\theta(x,y)}{\partial x}\text{ , }\psi^2(x,y) = \frac{\partial\theta(x,y)}{\partial y}, \tag{5}$$

where $\theta(x,y)$ is a smoothing function approximating the Gaussian.

The wavelet transform assumes that the input discrete image $S_1 f(x,y)$ is obtained by sampling a continuous 2-D function $f(x,y)$, smoothed at the finest scale:

$$S_1 f(n,m) = (f * \phi)(x,y)\,|_{x=n,y=n,(n,m)\in Z^2}\,, \tag{6}$$

where $\phi(x,y)$ is a smoothing scaling function and S is the approximation operator. The dilations of the two oriented wavelet functions at scale l are defined as:

$$\psi_l^i(x,y) = \frac{1}{l^2}\psi^i\left(\frac{x}{l},\frac{y}{l}\right)\Big|_{i=1,2} \tag{7}$$

The 2-D dyadic wavelet transform of a discrete image $S_1 f(x,y)$ is a uniform sampling of the continuous representation defined as:

ISSN: 1727-1983

$$\begin{Bmatrix} W^1_{2^J}(x,y) \\ W^1_{2^J}(x,y) \end{Bmatrix} = \begin{Bmatrix} f * \psi_{2^J}(x,y) \\ f * \psi_{2^J}(x,y) \end{Bmatrix} =$$

$$2^J \cdot \begin{Bmatrix} \frac{\partial}{\partial x}\left[f * \theta_{2^J}(x,y)\right] \\ \frac{\partial}{\partial y}\left[f * \theta_{2^J}(x,y)\right] \end{Bmatrix} = 2^J \cdot \vec{\nabla}(f * \theta_{2^J})(x,y), \quad (8)$$

$$S_{2^J} f(x,y) = 2^j \cdot f * \Phi_{2^J}(x,y), \quad (9)$$

where the maximum value of the coarsest (largest) dyadic scale j is equal to $\log_2(N)+1$ and $1 \le j \le J$ for a $N \times N$ input image.

Thus, the 2-D dyadic wavelet transform representation consists of the discrete coefficient images $\{W^1_{2^j}(n,m), W^2_{2^j}(n,m)\}$ which are proportional to the sampled horizontal and vertical components of the multiscale gradient vector $\vec{\nabla}(f * \theta_{2^j})(x,y)$ and the discrete approximation (smoothed) image $S_{2^J} f(n,m)$. Since the coefficient subimages have the same dimension as the original image, no sub-sampling of the wavelet coefficients was performed.

The original image can be exactly reconstructed using the inverse 2-D dyadic wavelet transform. The image gradient magnitude is related to the contrast values since the magnitude expresses the relative change of image intensity at each point.

The linear transformation function in RDWT linear stretching extends linearly the multiscale gradients. In this way, all regions of the image are enhanced similarly. For an image decomposed at J scales, the enhanced gradient magnitudes are given as:

$$M^e_s(n,m) = k_s M_s(n,m), \quad (10)$$

where $M^e_s(m,n)$ is the enhanced value of the gradient magnitude at position (m,n) of the scale s and k_s is the stretching factor $k_s > 1$ which could vary in different scales in order to improved structures or features of different sizes. For simplicity k_s was set equal to 20 for all scales.

The wavelet transform shrinkage methodology is a nonlinear transformation function used to improve mainly the contrast of low-contrast features. Utilizing different gain parameter values in the scales, the contrast of the structures with specific size is enhanced. In RDWT shrinkage methodology for denoising, the wavelet coefficients are set equal to zero when their magnitude is less than a threshold:

$$M^d_s(n,m) = \begin{cases} k_s M_s(n,m), & M_s(n,m) > T_s \\ 0, & otherwise \end{cases}, \quad (11)$$

where $M^d_s(n,m)$ are the modified magnitude gradients, k_s is the gain parameter and T_s is the threshold at scale s. We have chosen $k_s = 10$ and $T_s = 60$ for all scales.

The last RDWT approach is the one in which a background approximation is utilized. In the specific approach in addition to the 2nd and 3rd wavelet levels, a proportion of the coarse information included in the 4th wavelet decomposition level is utilized. The additional level contains large structures such as the breast tissue area, a possible high density region and the background area.

The CAD system

The system is presented in Ref. [9], however, here a short description is given. The segmentation module of the CAD system makes use of morphological and intensity-based functions aiming at the description of mammogram objects which are probable microcalcifications. For each individual object and related clusters, 54 features related with the intensity, shape and textural properties are initially extracted. A feature selection procedure, based on ROC analysis, resulted in the selection of the most discriminative feature set consisting of 22 features. In this work, the same feature set was utilized for the analysis of all the enhanced mammograms even though the discrimination power of each feature might change after the enhancement process.

The classification system that was employed for the reduction of the false positive findings was a feedforward backpropagation multilayer perceptron. Its architecture includes two hidden layers composed of 15 and 10 sigmoid nodes, respectively. However, due to the high dimensionality of the feature vector, principal component analysis (PCA) was employed to eliminate the features that contribute less than 3% to the total variation of dataset. After the PCA feature reduction procedure, the feature vector was fed to the neural network classifier which was trained using a quasi-Newton, one-step secant (OSS) algorithm. A two-fold cross validation methodology was used as a validation procedure. The overall performance of the CAD system was the average of the performances on the test sets from both data folds. The performance was evaluated using the area (A_Z) under ROC curve. The network training and testing processes were repeated ten times (with different initial conditions) measuring the network's reproducibility. For each series, the maximum, average and the standard deviation value of A_Z were calculated. These measures provide useful details about the performance and the stability of the neural network classifier.

The mammographic databases are the MIAS [10] and the Nijmegen [11] databases. The first contains 20 mammograms (spatial resolution: 50 μm, grey depth: 8 bits) including 205 annotated microcalcification clusters. The Nijmegen database consists of 40 mammograms (spatial resolution: 100 μm, grey depth: 12 bits) containing 105 annotated microcalcification clusters. To overcome the resolution difference a resampling technique is followed converting the resolution of the second database to 50 μm.

ISSN: 1727-1983

Results

Each enhancement technique is applied to the original mammogram. The segmentation and the feature extraction procedure takes as input the enhanced mammogram. The LRM technique resulted in the highest detection performance for both databases.

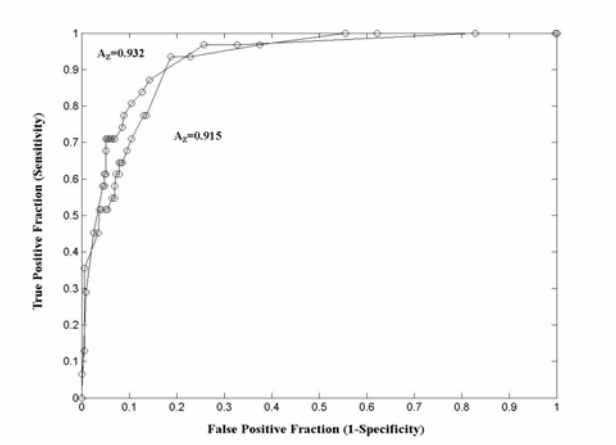

Figure 1. Receiver operating characteristic curves for the LRM enhancement methodology for both databases.

For the Nijmegen database the achieved score is A_Z=0.932 and for the MIAS database is A_Z=0.915 (Fig. 1). The detection performance of the CAD system for each enhancement technique is reported in Table 1. In this table, the performance of the CAD system without the utilization of the enhancement technique is also presented.

Enhancement Methodology	Databases	
	MIAS (A_Z)	Nijmegen (A_Z)
Without enhancement	0.866	0.825
LRM	0.932	0.915
CLAHE	0.837	0.802
RDWT Linear stretching	0.916	0.904
RDWT 2nd, 3rd & Background	0.891	0.887
RDWT Shrinkage	0.841	0.828

Table 1. The performance of the CAD system with the use of enhancement techniques for both mammographic datasets.

The enhancement methodologies, in most cases, result in the improvement of the detection ability of the CAD system. In addition to the LRM's performance, the RDWT stretching and the RDWT of the 2nd, 3rd and the approximation of background achieved higher detection scores than the performance of the unenhanced mammography.

The RDWT stretching A_Z scores are 0.916 and 0.904 for MIAS and Nijmegen databases, respectively. A lower score, 0.891 for MIAS and 0.887 for Nijmegen databases, is obtained when the RDWT methodology utilizes selective reconstruction of the 2nd and the 3rd decomposition levels and approximation of the background. The CLAHE and the RDWT shrinkage technique provided lower A_Z values compared to the score of the system without enhancement.

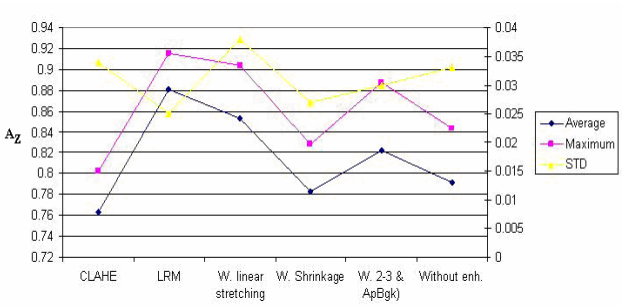

Figure 2. Maximum, average and STD A_Z values for the proposed enhancement techniques.

The average, maximum and STD for A_Z for the proposed preprocessing methods, for both mammographic databases, are depicted in Fig. 2. The LRM technique results in the highest maximum A_Z value and average A_Z values. These scores are obtained with the lowest STD values of the A_Z scores, a fact which increases the reliability of the enhancement process based on its high detection stability. The lowest maximum and average A_Z scores and the highest STD value are obtained by CLAHE which seems to be ineffective in the enhancement of the microcalcification clusters.

Discussion

Microcalcification enhancement algorithms have been employed in the preprocessing module of a CAD system aiming at the improvement of its detection performance. The evaluation of our previously developed CAD system was measured by ROC analysis in two well known annotated mammographic databases, the MIAS and the Nijmegen databases. The CLAHE technique and the LRM algorithm were selected since they have been previously utilized in mammographic enhancement studies. Also, a 2-D redundant dyadic wavelet transform was utilized modifying the fraction of the coarseness and the detailed portion of the mammogram. By the selection of specific decomposition levels, mainly the 2nd and the 3rd, the microcalcifications contrast is improved. In addition, the linear stretching and wavelet shrinkage techniques, which are wavelet-based techniques, were examined. The use of this preprocessing module was followed by segmentation, feature extraction, and classification to reduce the false positive samples.

Our work demonstrated that LRM resulted in the highest detection performance in both mammographic databases. The second in performance enhancement

ISSN: 1727-1983

technique was the RDWT linear stretching algorithm that provided A_Z scores about 1.7% and 1.2% lower than those from the LRM case, for each database respectively. The RDWT shrinkage and the CLAHE techniques resulted in scores even lower than those achieved by the system without the utilization of the preprocessing stage. The first technique resulted in A_Z=0.841 and A_Z=0.828 for the MIAS and the Nijmegen databases, respectively while the other are resulted in A_Z=0.837 and A_Z=0.802, for the two databases, respectively. The RDWT background approximation approach reached higher A_Z scores than the unenhanced mammogram, but significantly lower (about 4.4%) than those achieved by the LRM methodology.

Many research groups have paid attention to the development of efficient CAD systems for the detection of microcalcification clusters in mammography. The evaluation of a specific module of the CAD system, such as the preprocessing stage, is very rare in CAD reports, but rather the overall CAD's detection performance is reported. In [8], the radiologist's most-preferred (49%) microcalcification enhancement method was the adaptive neighborhood contrast enhancement algorithm which is similar to LRM technique. A wavelet-based approach followed with the preference to 28% of the mammograms and the unenhanced mammogram version which is preferred in 13% of the cases. In another study reported by Hemminger et. al. [12], a histogram-based intensity windowing technique appeared superior to the CLAHE and to the unprocessed mammogram. Even though the above studies provide a systematic categorization of the enhancement techniques based on their detection ability direct comparisons of the efficiency of the enhancement methods is not feasible.

Conclusions

In this study five enhancement methodologies have been used to improve the performance of an already reported CAD system [9]. The best performance was achieved by the utilization of LRM and RDWT linear stretching wavelet-based techniques. The CAD system is evaluated using two of the most known mammographic datasets (MIAS and Nijmegen). Although the achieved detection performance is satisfactory, further analysis must be carried out using larger mammographic datasets. Further investigation is needed in order to specify the parameters of segmentation which influence the detection performance of the CAD system.

References

[1] PIZER S.M., AMBURN E.O.P., and AUSTIN JD (1987). 'Adaptive histogram equalization and its variations', *Comput. Vision Graphics Image Process,* **39**, pp.355-368

[2] LURE F.Y.M., JONES P.W. and GABORSI R.S. (1996) 'Multi-resolution unsharp masking technique for mammogram image enhancement'. *Proc. SPIE*. **2710**, pp.830-839

[3] MORROW W.M., PARANJAPE R.B., and RANGAYYAN R.M.. (1992) 'Region-based contrast enhancement of mammograms', *IEEE Trans Med Imaging,* **11**, pp.392-406

[4] STRICKLAND R.N., and HAHN H. (1996) 'Wavelet transforms for detecting microcalcifications in mammograms', *IEEE Trans Med Imaging,* **15**, pp**.**218-229

[5] MALLAT S., and ZHONG S. (1992) 'Characterization of signals from multiscale edges', *IEEE Trans Pattern Anal Mach Intell*, **14**,pp.710-732

[6] LI H., LIU K.J.R., and LO S.C.B. (1997) 'Fractal modelling and segmentation for the enhancement of microcalcifications in digital mammograms', *IEEE Trans Med Imaging,* **16**, pp.785-798

[7] CHENG H.D., and XU H. (2002). 'A novel fuzzy logic approach to mammogram contrast enhancement',*Inform. Sciences*, **148**,pp 167-184

[8] SIVARAMAKRISHNA R., OBUCHOWSKI N.A., CHILCOTE W.A., CARDENOSA G., and POWELL K.A.. 'Comparing the performance of mammographic enhancement algorithms: A preference study', *Am J Rad*, **175**, pp.45-51

[9] PAPADOPOULOS A., FOTIADIS D.I., and LIKAS A. (2002) 'An automatic microcalcification detection system based on a hybrid neural network classifier'. *Artif Intell Med* **25,** pp.149-167.

[10] SUCKLING J., PARKER J., DANCE D., ASTLEY S., HUTT I., and BOGGIS C,. (1994) 'The mammographic images analysis society digital mammogram database'. *Exerpta Medica*, **1069**, pp**.**375–8

[11] KASSEMEIJER N. (1993) 'Adaptive noise equalization and recognition of microcalcifications in mammography'. *Inter J Pattern Recog Artif Intel*, **7**, pp.1357–76

[12] HEMMINGER B.M., ZONG S., MULLER K.E., COFFEY C.S., DELUCA M.C., JOHNSTON R.E., and PISANO E.D. (2001) 'Improving the detection of simulated masses in mammograms through two different image-processing techniques'. *Acad Radiol*. **8**, pp.845-55

ISSN: 1727-1983